

## Highly Sensitive and Broadly Reactive Quantitative Reverse Transcription-PCR Assay for High-Throughput Detection of Rift Valley Fever Virus<sup>∇</sup>

Brian H. Bird,<sup>1,2</sup> Darcy A. Bawiec,<sup>1</sup> Thomas G. Ksiazek,<sup>1</sup>  
Trevor R. Shoemaker,<sup>1</sup> and Stuart T. Nichol<sup>1\*</sup>

Special Pathogens Branch, Division of Viral and Rickettsial Diseases, National Center for Infectious Diseases, Centers for Disease Control and Prevention, 1600 Clifton Road, MS G-14, Atlanta, Georgia 30329,<sup>1</sup> and University of California, Davis, School of Veterinary Medicine, Davis, California 95616<sup>2</sup>

Received 4 May 2007/Returned for modification 11 July 2007/Accepted 13 August 2007

**Rift Valley fever (RVF) virus is a mosquito-borne virus associated with large-scale epizootics/epidemics throughout Africa and the Arabian peninsula. Virus infection can result in economically disastrous “abortion storms” and high newborn mortality in livestock. Human infections result in a flu-like illness, with 1 to 2% of patients developing severe complications, including encephalitis or hemorrhagic fever with high fatality rates. There is a critical need for a highly sensitive and specific molecular diagnostic assay capable of detecting the natural genetic spectrum of RVF viruses. We report here the establishment of a pan-RVF virus quantitative real-time reverse transcription-PCR assay with high analytical sensitivity (~5 RNA copies of in vitro-transcribed RNA/reaction or ~0.1 PFU of infectious virus/reaction) and efficiency (standard curve slope = -3.66). Based on the alignments of the complete genome sequences of 40 ecologically and biologically diverse virus isolates collected over 56 years (1944 to 2000), the primer and probe annealing sites targeted in this assay are known to be located in highly conserved genomic regions. The performance of this assay relative to serologic assays is illustrated by testing of known RVF case materials obtained during the Saudi Arabia outbreak in 2000. Furthermore, analysis of acute-phase blood samples collected from human patients (25 nonfatal, 8 fatal) during that outbreak revealed that patient viremia at time of presentation at hospital may be a useful prognostic tool in determining patient outcome.**

Rift Valley fever (RVF) virus, family *Bunyaviridae*, genus *Phlebovirus*, is a mosquito-borne pathogen capable of causing explosive outbreaks of severe human and livestock disease throughout Africa and more recently in 2000 on the Arabian peninsula. RVF virus infections in humans are characterized by a mild self-limiting febrile illness that can in a small percentage (ca. 1 to 2%) of patients progress to more severe complications including hepatitis, delayed onset neurologic disease, retinitis, or a hemorrhagic syndrome with high mortality (10, 11). Economically disastrous livestock epizootics often precede the detection of human illness and have been recorded since the early 1900s (6, 8). Livestock epizootics usually manifest as sweeping “abortion storms” and high newborn mortality approaching 100% among sheep, goats, and cattle (3, 5).

Although low-level RVF activity most likely occurs throughout enzootic regions each year, the emergence of RVF virus in large epidemic and/or epizootic cycles is typically associated with unusually heavy rainfall and the emergence of the natural reservoir host, which is thought to be primarily transovarially infected *Aedes* spp., floodwater mosquitoes (9). During large epidemics and epizootics the high numbers of infected individuals can greatly strain the capacity of the public health and veterinary

infrastructure to provide rapid real-time diagnostic testing and basic medical care for infected individuals or animals.

The ability of RVF virus to cross international and natural boundaries is well documented. In 1979 RVF virus was identified for the first time outside of continental Africa on the island of Madagascar (13). In addition, on at least two separate occasions the virus has caused “virgin soil” outbreaks in previously unaffected countries. In 1977 RVF virus was recorded for the first time north of the Sahara desert in Egypt and resulted in a massive epizootic/epidemic during which greater than 200,000 people were estimated to have been infected (12). Later in 2000, the virus was isolated for the first time outside of Africa across the Red Sea in Saudi Arabia and Yemen (1). The potential of further introductions of RVF virus into previously unaffected countries via infected livestock importation, mosquito translocation, or human travel or through intentional release illustrate the need for safe and effective veterinary and human vaccines and broadly based pan-RVF virus real-time molecular diagnostic assays.

The tripartite negative-sense single-stranded RNA genome of RVF virus contains the small ambisense segment (S segment) encoding the nucleoprotein and the nonstructural proteins, the medium segment (M segment) encoding the polyglycoprotein precursors, and the large segment (L segment) containing the virus RNA-dependent RNA polymerase (14). Recent complete genome sequencing of multiple isolates of RVF virus revealed that the overall virus genomic diversity is low (~5%) at the nucleotide level (2). This previous work involved the complete genomic characterization of the S, M, and L seg-

\* Corresponding author. Mailing address: Special Pathogens Branch, Division of Viral and Rickettsial Diseases, National Center for Zoonotic, Vector-borne and Enteric Diseases, Centers for Disease Control and Prevention, 1600 Clifton Road, MS G-14, Atlanta, GA 30329. Phone: (404) 639-1115. Fax: (404) 639-1118. E-mail: stn1@cdc.gov.

<sup>∇</sup> Published ahead of print on 5 September 2007.

ments of 33 wild-type virus isolates collected from throughout Africa and Saudi Arabia spanning 56 years (1944 to 2000).

Although prior examples of real-time reverse transcription-PCR (RT-PCR) assays for RVF virus exist (4, 7), these have potentially problematic nucleotide mismatches in the annealing sites of their respective primer and probe regions. Nucleotide alignments of the primer and probe regions of these two assays revealed mismatches with 14 (4) or 27 (7) of the recently completed RVF virus genomes, respectively. In addition, a critical mismatch at the exact 3' terminus of the reverse primer utilized in reference 7 was identified with two separate RVF virus lineages. Taken together, these nucleotide differences may interfere with the overall efficiency of virus detection. In an effort to improve upon existing assays and exploit the recent large increase in genomic data available for RVF virus strains, we began work on developing broadly based real-time RT-PCR molecular diagnostic assays capable of detecting the entire known genomic spectrum of RVF virus with a minimal number of nucleotide mismatches in either the primer or probe regions.

We report here the development of a real-time quantitative RT-PCR (Q-RT-PCR) assay with high nucleotide conservation of both primer and probe regions among the 33 virus strains included in our previous work and 7 additional strains completed since the time of that publication for a total of 40 strains that, when coupled with high-throughput 96-well RNA extraction methods, allows for the rapid identification of infected patients and animals. This assay has demonstrated its capability for the highly sensitive and efficient detection of RVF virus from human clinical materials utilizing archived patient samples collected in Saudi Arabia during an outbreak of RVF during the year 2000. The rapid and high-throughput detection of human or livestock infection with RVF virus is a critical first step in the identification and eventual control of this significant pathogen during outbreak situations.

#### MATERIALS AND METHODS

**RVF virus biosafety and high-throughput RNA extraction.** All manipulations that involved live RVF virus were performed within a biosafety level 4 containment laboratory. Virus RNA was extracted from RVF virus-infected Vero E6 cell supernatant utilizing either Tripure reagent (Roche) added at a ratio of 6:1 and extracted according to the manufacturer's recommended protocols or using a high-throughput 96-well format ABI 6100 nucleic acid workstation (Applied Biosystems) according to an optimized virucidal RNA extraction protocol (16). After transfer into chaotropic virucidal lysis buffer, tubes or plates containing RVF virus supernatants were surface decontaminated and transferred into a biosafety level 2 laboratory for RNA extraction. Utilization of this high-throughput extraction protocol allows for the completion of a Q-RT-PCR run of 96 samples of clinical material in approximately 4.5 to 5 h under field working conditions.

**Primer and probe design and standard curve optimization.** Full-length complete genome sequence alignments of the S, M, and L RNA segments of 33 biologically and phylogenetically diverse RVF virus isolates identified previously (2), plus 7 additional RVF virus strains, were analyzed. A highly conserved genomic domain within the L segment spanning nucleotides 2800 to 3200 was identified (all numbering is relative to the GenBank entry, i.e., the antigenomic sense). Located within this region were several potential forward and reverse primer and probe annealing sites that obeyed basic real-time RT-PCR optimization guidelines with a minimum of nucleotide mismatches. To determine which of these potential primer-probe combinations were optimal for RVF virus genome detection, *in vitro* RNA transcripts of the L gene segment encompassing the annealing sites of these primers and probes were amplified from a cDNA plasmid containing the entire L segment of RVF virus strain ZH-501 described previously (2) according to the manufacturer's recommended protocols (T7 Riboprobe MAX kit; Promega). After *in vitro* transcription the cDNA plasmid

template was digested twice with DNase I (RNase-free; New England Biolabs). After digestion, the transcribed RNA was extracted by using an RNaid purification kit (Qbiogene) twice, followed by RNA purification on RNeasy columns (QIAGEN) according to the manufacturer's recommended protocols to remove any unincorporated nucleotides or small digested DNA fragments. After purification, the RNA was quantitated by using an experimentally determined optical density at 230 nm. The molar extinction coefficient based upon the exact nucleotide sequence of the L segment fragment *in vitro* transcript was calculated by using an online tool ([www.basic.northwestern.edu/biotools/oligocalc.html](http://www.basic.northwestern.edu/biotools/oligocalc.html)) to determine the exact copy number of transcript molecules per microliter. This *in vitro*-transcribed and purified RNA was then serially diluted 10-fold ( $10^{-1}$  to  $10^{-15}$ ) in nuclease-free H<sub>2</sub>O to generate a standard curve for the relative comparisons of the sensitivities of various potential primer-probe combinations and reaction conditions. Each serial dilution was run in replicates of eight for Q-RT-PCR amplification according to the optimized protocol described below. The following primer and probe set was determined to be optimal: RVFL-2912fwdGG (5'-TGAAAATTCCTGAGACACATGG-3'), RVFL-2981revAC (5'-ACTTCCTTGCATCATCTGATG-3'), and RVFL-probe-2950 (5'-CAATGTAAGGGGCTGTGTGGACTTGTG-3') labeled at the 5' end with the reporter dye FAM and at the 3' end with the quencher BHQ1. Details of the primer location and a nucleotide alignment of all 40 complete RVF virus L segments can be found in (Fig. 1A) The RVFL-2912fwdGG primer has a single internal mismatch with wild-type strain 2269/74 and the attenuated laboratory strain MP12. The RVFL-2981revAC primer has a single internal mismatch with wild-type strain SA51. These mismatches have proven to not significantly impact the detection of these RVF virus strains by this Q-RT-PCR assay (Fig. 1). A search of all sequences available in GenBank revealed no significant sequence matches of these primers and probe with any nontargeted RNA or DNA.

**cDNA synthesis and Q-PCR conditions.** Over multiple experiments we found that the highest analytical sensitivity was attained by using a two-step protocol for RVF virus RNA detection. The first step was comprised of total cDNA synthesis using random priming, followed by a second step of RVF virus-specific Q-PCR. Total cDNA synthesis was accomplished by using a high-capacity cDNA archive kit (Applied Biosystems) according to the manufacturer's recommended protocol. Briefly, 50  $\mu$ l of extracted total RNA was added to 50  $\mu$ l of a 2 $\times$  cDNA synthesis reaction mixture containing random primers (500 pmol). Samples were then incubated at 25°C for 10 min, followed by 60 min at 37°C. After cDNA synthesis, 10  $\mu$ l of total cDNA was added into a Q-PCR mixture containing 1  $\mu$ l (1,000 pmol) of the forward primer RVFL-2912fwdGG, 1  $\mu$ l (1,000 pmol) of the reverse primer RVFL-2981revAC, 1  $\mu$ l (100 pmol) of the fluorogenic probe RVFL-probe-2950, 25  $\mu$ l of the 2 $\times$  Universal Master Mix (Applied Biosystems), and nuclease-free H<sub>2</sub>O to a final volume of 50  $\mu$ l. The Q-PCR was carried out in an Applied Biosystems 7500 instrument with a heating profile of 50°C for 2 min and 95°C for 10 min, followed by 40 cycles of alternating temperature cycling of 95°C for 15 s and 60°C for 1 min. The remaining 90  $\mu$ l of total cDNA was stored at -70°C for archival purposes for subsequent retesting or use in other molecular diagnostic assays.

**Analytical sensitivity and specificity with stock RVF virus.** After optimization of primer and probe composition and reaction conditions with *in vitro*-transcribed RNA, we sought to determine the analytical sensitivity and efficiency of this assay by using RNA extracted from wild-type RVF virus strain ZH501 serially diluted in a variety of diluents, including cell culture medium commonly used in the preparation of RVF virus stocks (Dulbecco modified Eagle medium plus 10% fetal bovine serum [FBS]; Invitrogen), 100% FBS (Invitrogen), and normal human control serum. Stock RVF virus strain ZH501,  $1.7 \times 10^6$  PFU/ml, was serially diluted 10-fold to establish a standard curve in each respective diluent and then extracted in replicates of eight on a 6100 nucleic acid purification platform (Applied Biosystems) as described elsewhere (16). The limit of detection (LOD) was determined as the final dilution for which a cycling threshold value ( $C_T$ ) was determined. To ensure that phylogenetically distant RVF virus strains were detectable by this assay, RNA extracted from 21 diverse RVF virus strains collected over a period of 56 years from 1944 to 2000 representing all known virus lineages were amplified by Q-RT-PCR according to the above protocol. In addition to determine whether nonspecific annealing might yield false-positive results in total cellular RNA extracted from animal host species, the total RNA of tissue samples from bovine, ovine, human, rodent, and mosquito species were tested according to the Q-RT-PCR protocol described above.

**Q-RT-PCR assay validation with human clinical materials.** The human clinical specimens used in the present study were collected during an outbreak of RVF virus disease in Saudi Arabia in 2000. A total of 62 patient acute-phase blood samples collected from a total of 33 patients (25 nonfatal and 8 fatal outcomes) were tested. Of these, a total of 26 samples were single blood collections from 26 infected patients (20 nonfatal and 6 fatal outcomes) with a known date of collection after onset of

**A.**

**RVF strain Nucleotide Sequence and primer/probe position**

	2910	2920	2930	2940	2950	2960	2970	2980	2990	3000
1260/78	CCCCAATAAAG	TGAAAATTCC	TGAGACACATGG	CATCAGGGCTCG	GAAAGCAATGTA	AAGGGGCCTGT	TGGACTTGTG	CAACATCAGAT	GATGCAAGGAAGT	
1853/78	.....	.....	.....	.....	.....	.....	.....	.....	.....	.....
<b>2250/74*</b>	.....	.....	.....	.....	<b>C</b>	.....	.....	.....	.....	.....
<b>2269/74*</b>	.....	<b>C</b>	<b>G</b>	.....	<b>G</b>	.....	.....	.....	.....	.....
<b>2373/74*</b>	.....	<b>G</b>	.....	.....	<b>T</b>	.....	.....	<b>G</b>	.....	.....
<b>73HB1230*</b>	.....	.....	.....	.....	.....	.....	.....	.....	.....	.....
73HB1449	.....	.....	.....	.....	.....	.....	.....	.....	.....	.....
<b>74HB59*</b>	.....	.....	.....	.....	.....	.....	.....	.....	.....	.....
763/70	.....	<b>G</b>	.....	.....	<b>T</b>	.....	.....	.....	.....	.....
ANK3837	.....	.....	.....	.....	.....	.....	.....	.....	.....	.....
ANK6087	.....	.....	.....	.....	.....	.....	.....	.....	.....	.....
<b>ARD38388*</b>	.....	<b>G</b>	.....	.....	<b>T</b>	.....	<b>A</b>	.....	<b>T</b>	.....
<b>CARR1622*</b>	.....	.....	.....	.....	.....	.....	.....	.....	.....	.....
Clone13	.....	.....	.....	.....	.....	.....	.....	.....	.....	.....
<b>Entebbe*</b>	.....	<b>G</b>	.....	.....	<b>T</b>	.....	.....	.....	<b>G</b>	.....
<b>HvB375*</b>	.....	.....	.....	.....	.....	.....	.....	.....	.....	.....
Kenya IB8	.....	<b>G</b>	.....	.....	<b>T</b>	.....	.....	.....	.....	.....
Kenya57	.....	<b>G</b>	.....	.....	<b>T</b>	.....	<b>A</b>	.....	<b>G</b>	.....
<b>Kenya83*</b>	.....	.....	.....	.....	.....	.....	.....	.....	.....	.....
<b>Kenya98*</b>	.....	.....	.....	.....	.....	.....	.....	.....	.....	.....
<b>MgH824*</b>	.....	.....	.....	.....	.....	.....	.....	.....	<b>C</b>	.....
MP12	.....	.....	<b>A</b>	.....	.....	.....	.....	.....	<b>C</b>	.....
OS1	.....	<b>G</b>	.....	.....	<b>T</b>	.....	.....	.....	.....	.....
<b>OS3*</b>	.....	<b>G</b>	.....	.....	<b>T</b>	.....	.....	.....	.....	.....
<b>OS8*</b>	.....	<b>G</b>	.....	.....	<b>T</b>	.....	.....	.....	.....	.....
<b>OS9*</b>	.....	<b>G</b>	.....	.....	<b>T</b>	.....	.....	.....	.....	.....
SA51	.....	<b>G</b>	.....	.....	<b>T</b>	.....	.....	<b>G</b>	.....	<b>A</b>
<b>SA75*</b>	.....	<b>G</b>	.....	.....	<b>T</b>	.....	.....	.....	.....	.....
<b>Saudi-2000*</b>	.....	.....	.....	.....	.....	.....	.....	.....	.....	.....
Smithburn	.....	<b>G</b>	.....	.....	<b>T</b>	.....	.....	<b>G</b>	.....	.....
T46	.....	.....	.....	.....	.....	.....	.....	.....	.....	<b>C</b>
T1	.....	.....	.....	.....	.....	.....	.....	.....	.....	<b>C</b>
ZC3349	.....	.....	.....	.....	.....	.....	.....	.....	.....	<b>C</b>
<b>ZH1776*</b>	.....	.....	.....	.....	.....	.....	.....	.....	.....	<b>C</b>
ZH501 (900060)	.....	.....	.....	.....	.....	.....	.....	.....	.....	<b>C</b>
<b>ZH501*</b>	.....	.....	.....	.....	.....	.....	.....	.....	.....	<b>C</b>
<b>ZH548*</b>	.....	.....	.....	.....	.....	.....	.....	.....	.....	<b>C</b>
<b>Zinga*</b>	.....	.....	.....	.....	.....	.....	.....	.....	.....	.....
ZM657	.....	.....	.....	.....	.....	.....	.....	.....	.....	<b>C</b>
ZS6365	.....	.....	.....	.....	.....	.....	.....	.....	.....	<b>C</b>

**B.**

Primer/Probe	Sequence	Annealing Temp
RVFL-2912fwdgg :	5'-TGAAAATTCCTGAGACACATGG-3'	58
RVFL-2981revAC:	5'-ACTTCCTTGCATCATCTGATG-3'	57
RVFL-2950-Probe:	5'-(FAM)-CAATGTAAGGGGCCTGTGTGGACTTGTG-(BHQ1)-3'	72

FIG. 1. (A) Alignment of nucleotides 2900 to 3001 of RVF virus L segments from 40 different virus strains. Nucleotide identities throughout the alignment with wild-type strain 1260/78 are indicated by a dot (.) (GenBank accession numbers DQ375395 to DQ375434). The positions of primers RVFL-2912ggfwd and RVFL-2981revAC and fluorogenic probe RVFL-probe-2950 are indicated in underlined red text. The 21 phylogenetically diverse strains tested by Q-RT-PCR amplification are indicated by a boldfaced strain name and an asterisk. All RVF virus strains tested were positively detected by this assay. Note the high nucleotide conservation at the primer-probe annealing sites among these 40 RVF virus strains. (B). Nucleotide sequence of the primer-probe combination of RVFL-2912ggfwd, RVFL-2981revAC, and RVFL-probe-2950 and their respective calculated annealing temperatures using an online calculator (<http://www.basic.northwestern.edu/biotools/oligocalc.html>).

clinical symptoms. A subset of samples (36) contained serial blood collections from a total of seven patients (five nonfatal and two fatal outcomes) that were obtained on multiple days after the onset of clinical symptoms until either the patient's recovery or death due to RVF disease. For all specimens tested, the final patient outcome and day after onset of symptoms at the time of sample collection were known. For validation purposes, the results from this pan-RVF virus Q-RT-PCR were compared to earlier results of antigen capture, immunoglobulin M (IgM) and IgG serological testing (10, 15).

**Statistical testing.** Patient data were grouped into fatal versus nonfatal cases and groups were further defined by the day after the onset of clinical symptoms (days 1 to 4, 5 to 8, and 9 to 14). These were then analyzed by univariate analysis

of variance and a post hoc Tukey's test with an  $\alpha$ -level set at 0.05. All statistical testing was completed with SPSS v.12.0 (LEAD Technologies).

**RESULTS**

**Primer and probe design.** After analysis of the complete genomes (S, M, and L segments) of 40 biologically and ecologically diverse RVF virus strains, a highly conserved region was identified on the virus L segment at approximately nucle-

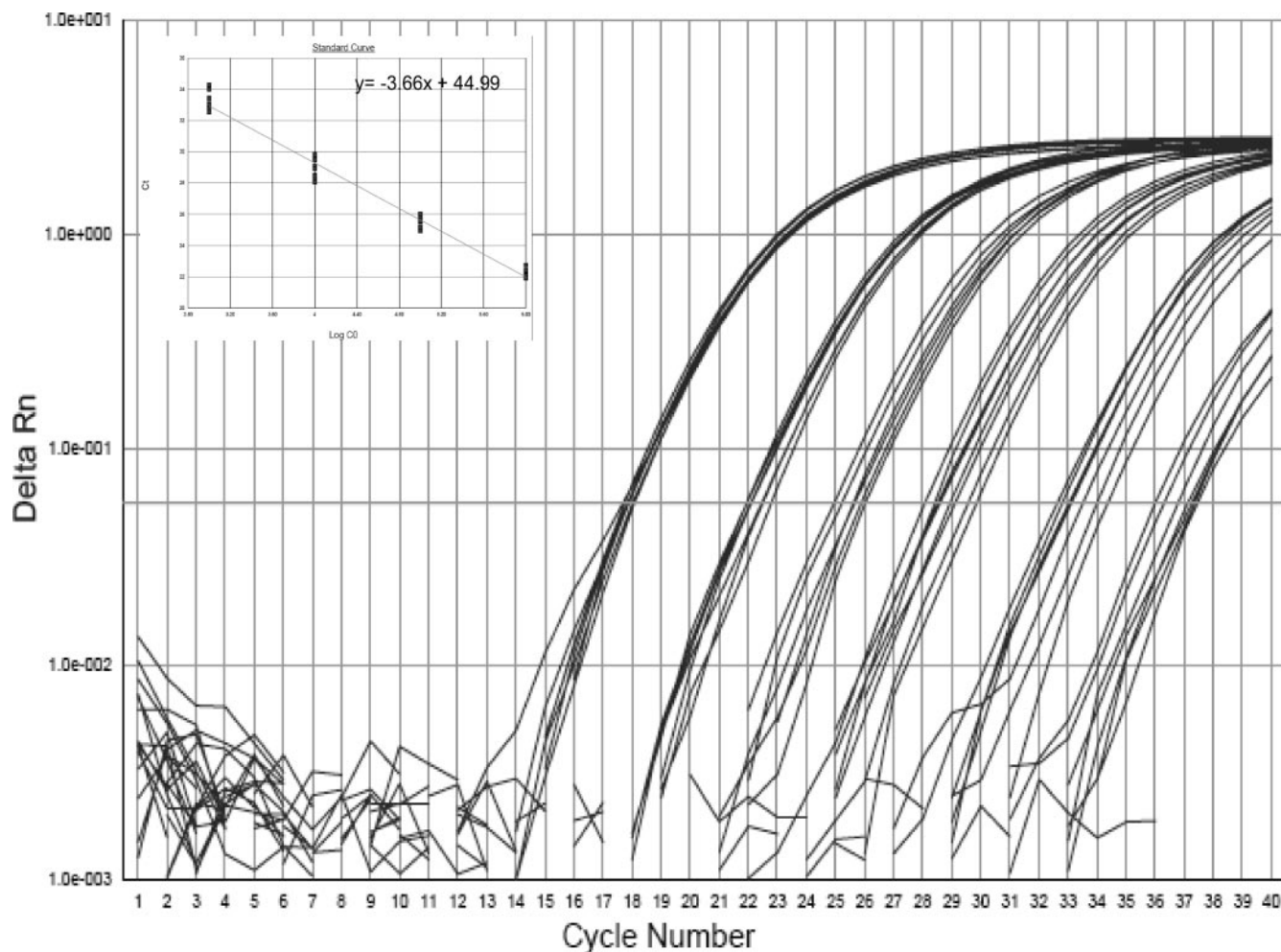


FIG. 2. Delta Rn (change in fluorescence) versus cycle number. The results of Q-RT-PCR amplification of RVF virus stock strain ZH501 diluted serially 10-fold ( $10^{-1}$  to  $10^{-8}$ ) in serum are depicted in the main chart. The inset shows the results of a log transformation of the  $C_T$  values plotted versus  $\log_{10}$  dilutions of extracted RNA of stock ZH501. The resulting equation of the standard curve was  $y = -3.66x + 44.99$ . The LOD of this assay with serially diluted stock virus in serum was approximately 0.1 PFU/rxn.

otide positions 2800 to 3200. Careful analysis of this region identified multiple potential annealing sites of primer and probe combinations that followed basic rules of real-time PCR design. A total of six sets spanning this region were designed and tested with the set (RVFL-2912fwdGG, RVFL-2981revAC, and RVFL-probe-2950) demonstrating the greatest analytical sensitivity, efficiency, and highest nucleotide conservation. A nucleotide alignment of the 40 RVF virus strains and the location of this primer and probe set can be found in Fig. 1.

**Optimization of Q-RT-PCR assay analytical sensitivity.** Using purified in vitro-transcribed RNA from the RVF virus L segment as a template, we were able to optimize reaction conditions and to determine the LOD of this assay. After multiple experiments comparing single-step (RT and Q-PCR in a single tube) or two-step (RT and Q-PCR in separate tubes), it was found that the overall analytical sensitivity was reduced after a single-step protocol (data not shown). Subsequently, all further assay optimization was carried out using a two-step protocol with RT and Q-PCR occurring separately to

allow for optimal buffering conditions to be available for each enzyme mixture. Multiple primer-probe sets were initially designed centering on a region of high nucleotide identity found on the RVF virus L segment among all 33 RVF virus complete genomes published previously (2), plus 7 additional strains more recently completed. Using in vitro-transcribed RNA as an input template, it was determined that one set was significantly more sensitive than the others in detecting RVF virus. Using serial 10-fold dilutions of transcribed RNA to establish a standard curve, it was experimentally determined that the LOD of the optimized Q-RT-PCR assay was approximately 5 genome copies per reaction and that this set yielded a slope of  $-3.58$  when  $C_T$  values were plotted versus  $\log_{10}$  dilutions of RNA (data not shown). After optimization using highly purified transcribed RNA, further analytical sensitivity and amplification efficiency testing was completed with RVF virus strain ZH501 stock serially diluted 10-fold ( $10^{-1}$  to  $10^{-8}$ ) in replicates of eight in either cell culture supernatant (Dulbecco modified Eagle medium plus 10% FBS), 100% FBS, or normal control human serum. After RNA extraction, these dilutions

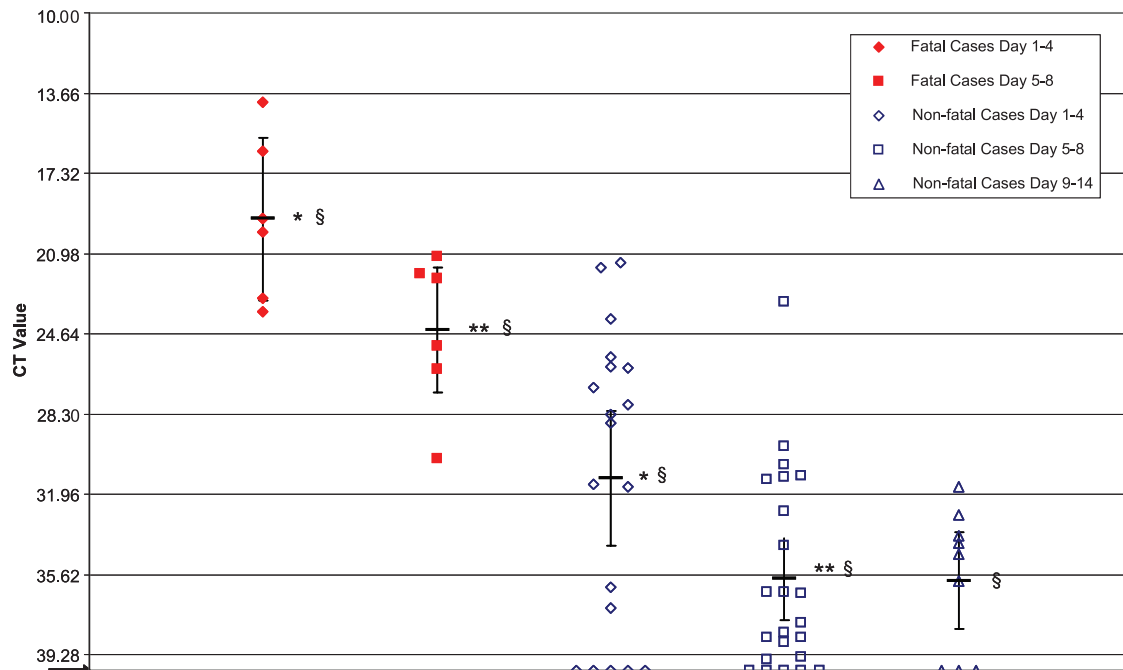


FIG. 3. RVF RNA load among patients with fatal and nonfatal outcomes. Results of Q-RT-PCR amplification of RVF virus-infected patient sera collected during the epidemic/epizootic in Saudi Arabia in 2000. A total of 62 patient specimens are divided into groups according to patient outcome (nonfatal or fatal) and by days after onset of clinical symptoms (days 1 to 4, 5 to 8, and 9 to 14). Significant differences ( $P < 0.001$ ) between the mean  $C_T$  value of fatal and nonfatal groups at days 1 to 4 postinfection are indicated by a single asterisk (\*) and at days 5 to 8 by a double asterisk (\*\*). At all time points the mean RVF RNA load of fatal cases was significantly higher ( $P < 0.001$ ) than nonfatal cases and is indicated by a “§” symbol. Note that the mean serum RVF RNA load of both fatal and nonfatal cases decrease as the time after onset increases, presumably due to the development of anti-RVF virus-specific IgM and/or IgG antibody with the subsequent clearance of virus from patient blood. Error bars indicate the mean value  $\pm 2$  standard errors of the mean. The LOD of the Q-RT-PCR assay is indicated by an arrow and represents a  $C_T$  value of  $>40$ . The scale of the y-axis scale is demarcated every 3.66  $C_T$  values, which corresponds to a  $1.0 \log_{10}$  PFU/ml change in virus RNA titer as calculated from titration of the stock RVF virus.

were used to establish a standard curve as described above to determine the LOD in control serum of ( $\sim 0.1$  PFU/reaction [rxn]) and amplification efficiency (slope =  $-3.66$ ) of the Q-RT-PCR assay (Fig. 2). To determine the robustness of this technique in the detection of a diverse array of RVF virus strains, a total of 21 RVF virus isolates were tested to ensure detection. Using total RNA extracted from infected cell culture supernatants, all 21 phylogenetically diverse strains were detected (Fig. 1). To ensure that no false-positive or “off-target” results could be generated due to nonspecific annealing with the total RNA of several potential host species, the total RNA of bovine, ovine, mouse, rat, mosquito, and human tissues were tested. As expected, in all cases, the total RNAs were negative and equivalent to no-template controls (data not shown).

**Validation with human RVF clinical materials.** A total of 62 RNA samples extracted from previously diagnosed patient sera representing a total of 33 patients (25 nonfatal and 8 fatal) were used to validate and compare the utility of the proposed Q-RT-PCR assay with standard serological assays (antigen capture, IgM antibody, and IgG antibody) used for RVF diagnosis. A significant difference was found between patient RVF virus RNA load, as reflected by mean Q-RT-PCR  $C_T$  values, between fatal and nonfatal cases at days 1 to 4 (mean  $C_T$  values: fatal = 19.4, nonfatal = 31.2;  $P < 0.001$ ), days 5 to 8 (mean  $C_T$  values: fatal = 24.5, nonfatal = 35.8;  $P < 0.001$ ), and

days 9 to 14 (mean  $C_T$  value: nonfatal = 35.9;  $P < 0.001$ ) after the onset of clinical symptoms (Fig. 3). Among nonfatal cases significant decreases in patient RVF RNA load were detected between days 1 to 4 and between days 5 to 8 ( $P < 0.05$ ). Interestingly, in nonfatal cases, samples collected at days 5 to 14 after onset of symptoms were often positive only for the presence of RVF specific antibody or demonstrated very low levels of RVF virus-specific RNA, presumably reflecting the clearance of virus from patient blood to levels below the Q-RT-PCR detection threshold (Fig. 3 and data not shown).

To investigate the dynamics of the Q-RT-PCR and serologic assay results relative to time after onset of illness, serial bleeds from multiple patients (five nonfatal and two fatal) were analyzed. The results for four representative patients (two nonfatal and two fatal) are illustrated in Fig. 4. As expected, and in concordance with the serologic assays, the Q-RT-PCR assay correctly identified the acutely infected patient specimens. Among the serially sampled nonfatal cases, IgM and IgG  $SUM_{OD}$  (adjusted optical density) values were found to increase over time, while a corresponding decrease was observed in both RVF antigen capture  $SUM_{OD}$  and RVF virus RNA load, as measured by Q-RT-PCR  $C_T$  values. In these nonfatal cases, RVF antigen capture values decreased to negative levels at least 5 days prior to the loss of detectable Q-RT-PCR signals. In all nonfatal cases both RVF antigen capture and Q-RT-PCR RVF RNA load began to decrease (days 1 to 4)

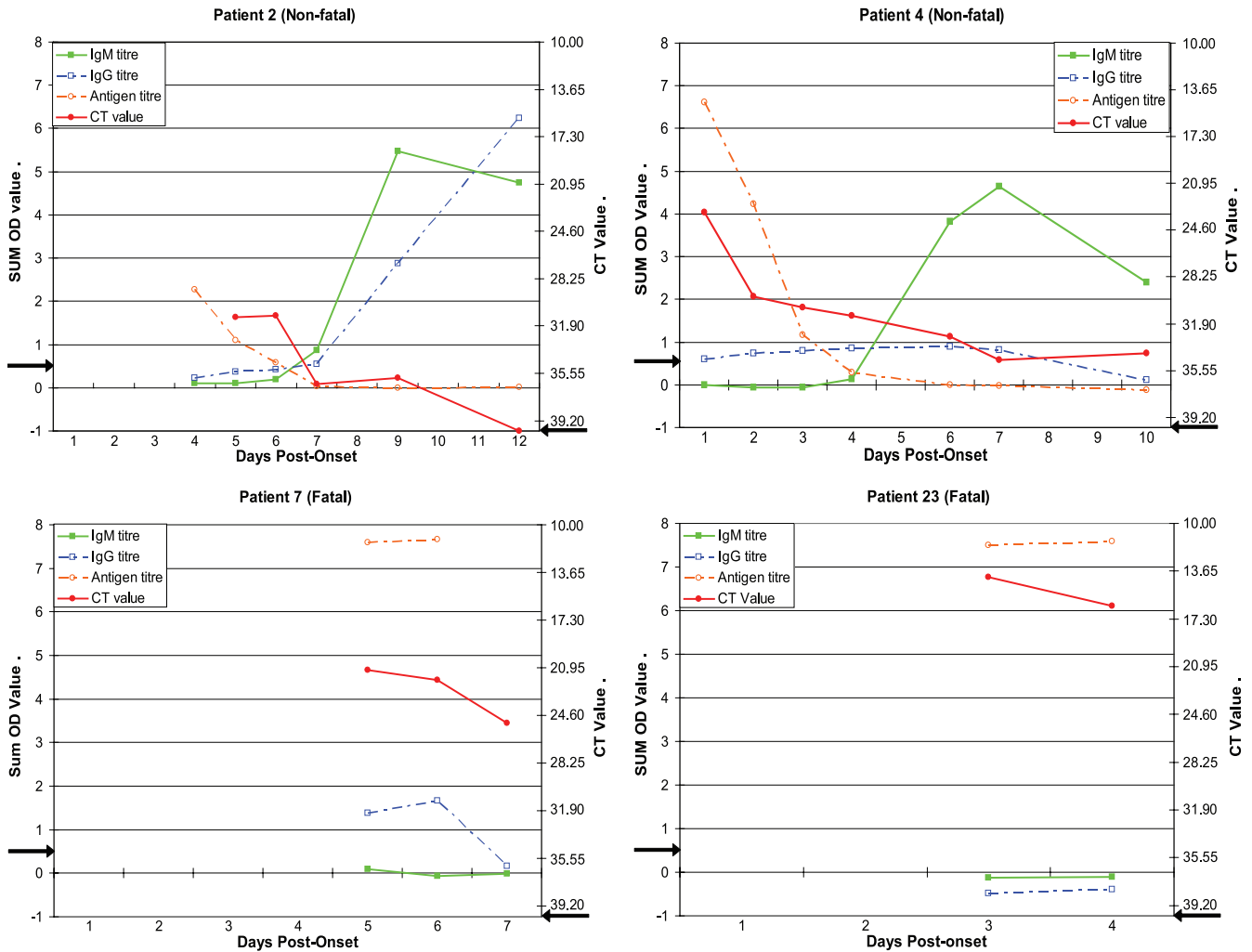


FIG. 4. Results of Q-RT-PCR and RVF virus-specific antigen capture, IgM, and IgG ELISAs of a representative subset of four human patients from whom multiple blood samples were obtained. Patients 2 and 4 represent nonfatal outcomes of RVF. Patients 7 and 23 represent fatal outcomes of RVF. IgM, solid square and solid line; IgG, open square and dashed line; antigen capture, open circle and dashed line; Q-RT-PCR  $C_T$  values, closed circle and solid line. All serological data are expressed as the adjusted  $SUM_{OD}$  of four sample dilutions of 1:4, 1:16, 1:64, and 1:256 for the anti-RVF antigen capture assay and dilutions of 1:100, 1:400, 1:1,600, and 1:6,400 for the anti-RVF specific IgM and IgG assays. The LOD of the Q-RT-PCR assay is indicated by an arrow and represents a  $C_T$  value of  $>40$ . The scale of the right-hand y-axis scale is demarcated every 3.66 U, which corresponds to a 1.0  $\log_{10}$  PFU/ml change in virus RNA titer as calculated from titration of stock RVF virus.

before significant increases in RVF specific IgM and IgG were detected, a result likely due to the lack of circulating free anti-RVF IgM or IgG available for detection early in the course of infection. In contrast, the two serially sampled fatal cases had extremely high RVF antigen capture and low Q-RT-PCR  $C_T$  values by days 3 to 5 after onset of illness, with no significant levels of anti-RVF specific IgM or IgG antibody. Importantly, the level of patient virus load among these fatal cases (as measured by RVF antigen capture and Q-RT-PCR) did not appear to decrease significantly during the follow-up period.

**DISCUSSION**

The central feature of real-time PCR-based diagnostic techniques is the high analytical sensitivity and specificity afforded by unique primer and probe sites located on genomic nucleic

acid templates. Unfortunately, many important human and veterinary pathogens have significant genome nucleotide variation across their known strain diversity that renders the design of broadly reactive and highly sensitive primers and probes problematic. Recent analysis of the complete genome sequence of 40 biologically and ecologically diverse RVF virus strains demonstrated that the overall nucleotide diversity of RVF virus is low as the result of recent common ancestry (2). This data set laid the foundation for the successful establishment of a rapid and high-throughput technique for the real-time Q-RT-PCR detection of the entire known genomic diversity of RVF virus.

Using a single primer and probe set annealing in a highly conserved domain located on the virus L segment, we successfully developed an assay with excellent analytical sensitivity (~5 genome copies/rxn or ~0.1 PFU/rxn) that performed well in the detection of RVF virus in vitro-transcribed and whole

stock virus extracted RNA template, respectively (Fig. 2). The highly sensitive and quantitative nature of this assay should be of great benefit in experimental settings as a research tool useful in monitoring virus loads in animal models of RVF virus disease. In addition, the successful detection of 21 phylogenetically diverse RVF virus strains representative of all known virus lineages (Fig. 1) confirmed the highly conserved nature of the primer and probe annealing sites. The utility of the assay relative to standard serologic assays was validated using human patient sera collected during the year 2000 outbreak of RVF virus in Saudi Arabia (10, 15). A total of 62 samples from 33 patients (25 nonfatal and 8 fatal cases) were identified for which prior laboratory testing results were available and sufficient volumes remained to allow RNA extraction and Q-RT-PCR testing. Unfortunately, no other individually or serially collected specimens with a known patient outcome were available. As expected, the mean overall patient RVF virus RNA load was found to be significantly lower in nonfatal patients than in those with fatal outcomes. Interestingly, even though the RVF virus RNA load was high initially among some nonfatal cases, we found significant decreases in mean RNA load between days 1 to 4 and days 5 to 8 after the onset of symptoms (Fig. 3). The combination of these data with the rapid decreases in RNA load observed among serially sampled nonfatal cases (Fig. 4) suggests that testing of serial patient specimens collected 24 to 48 h apart may have prognostic utility in determining the progression of RVF virus disease and ultimately patient outcome. Overall, the dynamics of RVF virus infection in the nonfatal cases examined here revealed that the duration of detectable patient viremia or RNAemia (virus RNA per milliliter of blood) (as detected by either antigen capture enzyme-linked immunosorbent assay [ELISA] or Q-RT-PCR, respectively), was relatively brief, and their decrease coincided with detectable increases in RVF specific IgM and IgG antibody levels (Fig. 4).

These results suggest that the "window of opportunity" for detection by RVF specific antigen capture ELISA may be limited to be approximately 1 to 7 days after the onset of clinical symptoms in human patients. Due to its higher detection capability, Q-RT-PCR may remain of diagnostic value up to at least day 10 after the onset of symptoms. However, it is apparent from this data set that the diagnostic value of Q-RT-PCR decreases significantly past day 10 after the onset of symptoms. These findings taken together highlight the complementary nature of molecular detection assays and serologic tests and the importance of using a combination of assays for reliable diagnosis of virus infection. Epidemiologic investigations of outbreaks occurring in regions with endemic RVF virus activity are often complicated by the fact that a percentage of individuals will have had prior exposure to RVF virus. Use of both antibody and virus detection assays can provide insights into disease status by, for example, differentiating between an enzootic versus epizootic region or between an acute-versus convalescent-phase individual. For instance, the presence of RVF virus-specific IgG alone without virus-specific IgM antibody or evidence of acute viremia (antigen capture or Q-RT-PCR) is highly suggestive that the infection occurred at some time previously and is not the result of recent virus exposure. In addition, during outbreak investigations, information regarding such things as the time after the onset of illness

are often not available to the testing laboratory or do not accompany specimens. The absence of this information and of antibody testing may result in false-negative reporting of late acute-stage and convalescent individuals or animals.

Comparison of the fatal and nonfatal cases revealed a striking difference in the levels of virus detected in the blood. Mean virus RNA levels were elevated up to 10  $C_T$  values ( $\sim 3 \log_{10}$  PFU equivalents/ml) upon initial sampling of fatal cases relative to those that went on to survive. In addition, little decrease in virus RNA or virus antigen levels was observed prior to the death of these patients, presumably due to the high replication of the virus in the virtual absence of detectable anti-RVF virus IgM or IgG antibody (Fig. 3 and 4). Further studies will be necessary, but these findings based on a relatively limited number of patients suggest that measurement of initial patient virus loads may help identify high-risk patients, especially if follow-up samples can be obtained. Currently, the host specific risk factors for RVF virus mortality are not understood, and early indicators such as viral load may shed light on this important topic. Given that outbreaks frequently occur in rural areas of Africa, affecting very large numbers of individuals (for instance the Egyptian outbreak in 1977 to 1978 was estimated to have involved >200,000 human infections), the rapid identification of high-risk patients can have practical implications for patient management in these resource-limited settings.

High-throughput real-time molecular detection assays are critical for the rapid identification of acutely infected individuals or animals during potentially explosive RVF virus epizootics or epidemics. Here we establish a rapid, highly sensitive, and robust method of Q-RT-PCR capable of detecting the entire known genomic sequence diversity of RVF virus. Recently, the utility of this assay was illustrated further when it was successfully used under field conditions in the diagnostic testing of more than 1,000 specimens from acutely infected livestock herds during the recent large RVF epidemic/epizootic that occurred in eastern Africa (Kenya, Somalia, and Tanzania) during late 2006 and early 2007 (unpublished data). This validated and field-tested assay should have great utility in the diagnosis of acute cases during outbreaks of infection among humans and animals during naturally occurring outbreaks or after intentional release into previously unaffected areas.

#### ACKNOWLEDGMENTS

We thank Beth Vitalis, Shea Gardner, and Tom Slezak of the Lawrence Livermore National Laboratory, Livermore, CA, for initial input regarding RVF signature analysis. We also thank Marina Khristova for excellent assistance in generating complete genome RVF virus sequence data and Jonathan Towner and César Albariño and Tara Sealy for helpful comments and support during the completion of these studies.

B.H.B. was supported during the completion of this study by the Oak Ridge Institute for Science and Education, Oak Ridge, TN; a Student's Training in Advanced Research fellowship; and the Veterinary Scientist Training Program of the University of California at Davis School of Veterinary Medicine (UCDSVM). B.H.B. thanks N. James MacLachlan of the UCDSVM for steadfast support and mentoring throughout the completion of this study.

The findings and conclusions in this report are those of the authors and do not necessarily represent the views of the funding agency.

## REFERENCES

1. **Anonymous.** 2000. Update: outbreak of Rift Valley Fever—Saudi Arabia, August–November 2000. *Morb. Mortal. Wkly. Rep.* **49**:982–985.
2. **Bird, B. H., M. L. Khristova, P. E. Rollin, T. G. Ksiazek, and S. T. Nichol.** 2007. Complete genome analysis of 33 ecologically and biologically diverse Rift Valley fever virus strains reveals widespread virus movement and low genetic diversity due to recent common ancestry. *J. Virol.* **81**:2805–2816.
3. **Coetzer, J. A.** 1977. The pathology of Rift Valley fever. I. Lesions occurring in natural cases in new-born lambs. *Onderstepoort J. Vet. Res.* **44**:205–211.
4. **Drosten, C., S. Gottig, S. Schilling, M. Asper, M. Panning, H. Schmitz, and S. Gunther.** 2002. Rapid detection and quantification of RNA of Ebola and Marburg viruses, Lassa virus, Crimean-Congo hemorrhagic fever virus, Rift Valley fever virus, dengue virus, and yellow fever virus by real-time reverse transcription-PCR. *J. Clin. Microbiol.* **40**:2323–2330.
5. **Easterday, B. C., M. H. McGavran, J. R. Rooney, and L. C. Murphy.** 1962. The pathogenesis of Rift Valley fever in lambs. *Am. J. Vet. Res.* **23**:470–479.
6. **Findlay, G. M. D. R.** 1931. The virus of Rift Valley fever or enzootic hepatitis. *Lancet* **ii**:1350–1351.
7. **Garcia, S., J. M. Crance, A. Billecocq, A. Peinnequin, A. Jouan, M. Bouloy, and D. Garin.** 2001. Quantitative real-time PCR detection of Rift Valley fever virus and its application to evaluation of antiviral compounds. *J. Clin. Microbiol.* **39**:4456–4461.
8. **Kabete Veterinary Laboratories.** 1910. Diseases of sheep. Kenya Veterinary Department annual report 1910. Kenyan Department of Veterinary Services, Nairobi, Kenya.
9. **Linthicum, K. J., A. Anyamba, C. J. Tucker, P. W. Kelley, M. F. Myers, and C. J. Peters.** 1999. Climate and satellite indicators to forecast Rift Valley fever epidemics in Kenya. *Science* **285**:397–400.
10. **Madani, T. A., Y. Y. Al-Mazrou, M. H. Al-Jeffri, A. A. Mishkhas, A. M. Al-Rabeah, A. M. Turkistani, M. O. Al-Sayed, A. A. Abodahish, A. S. Khan, T. G. Ksiazek, and O. Shobokshi.** 2003. Rift Valley fever epidemic in Saudi Arabia: epidemiological, clinical, and laboratory characteristics. *Clin. Infect. Dis.* **37**:1084–1092.
11. **McIntosh, B. M., D. Russell, I. dos Santos, and J. H. Gear.** 1980. Rift Valley fever in humans in South Africa. *S. Afr. Med. J.* **58**:803–806.
12. **Meegan, J. M.** 1981. Rift Valley fever in Egypt: an overview of the epizootics in 1977 and 1978. *Contrib. Epidemiol. Biostat.* **3**:114–123.
13. **Morvan, J., P. E. Rollin, S. Laventure, I. Rakotoarivony, and J. Roux.** 1992. Rift Valley fever epizootic in the central highlands of Madagascar. *Res. Virol.* **143**:407–415.
14. **Schmaljohn, C. S., and J. W. Hooper.** 2001. *Bunyaviridae*: the viruses and their replication, p. 1581–1602. *In* D. M. Knipe and P. M. Howley (ed.), *Fields virology*, 4th ed. Lippincott-Raven Publishers, Philadelphia, PA.
15. **Shoemaker, T., C. Boulianne, M. J. Vincent, L. Pezzanite, M. M. Al-Qahtani, Y. Al-Mazrou, A. S. Khan, P. E. Rollin, R. Swanepoel, T. G. Ksiazek, and S. T. Nichol.** 2002. Genetic analysis of viruses associated with emergence of Rift Valley fever in Saudi Arabia and Yemen, 2000–01. *Emerg. Infect. Dis.* **8**:1415–1420.
16. **Towner, J. S. S., T. K. Sealy, T. G. Ksiazek, and S. T. Nichol.** High-throughput molecular detection of hemorrhagic fever virus threats with applications for outbreak settings. *J. Infect. Dis.*, in press.